2009

The mitogen-activated protein kinase scaffold KSR1 Is required for recruitment of extracellular signal-regulated kinase to the immunological synapse

Emanuele Giurisato
Washington University School of Medicine

Joseph Lin
Washington University School of Medicine

Angus Harding
Washington University School of Medicine

Elisa Cerutti
Washington University School of Medicine

Marina Cella
Washington University School of Medicine

See next page for additional authors

Molecular and Cellular Biology

The Mitogen-Activated Protein Kinase Scaffold KSR1 Is Required for Recruitment of Extracellular Signal-Regulated Kinase to the Immunological Synapse

Emanuele Giurisato, Joseph Lin, Angus Harding, Elisa Cerutti, Marina Cella, Robert E. Lewis, Marco Colonna and Andrey S. Shaw

Mol. Cell. Biol. **2009, 29(6):1554. DOI: 10.1128/MCB.01421-08.**
Published Ahead of Print 12 January 2009.

MOLECULAR AND CELLULAR BIOLOGY, Mar. 2009, p. 1554–1564 Vol. 29, No. 6
0270-7306/09/$08.00+0 doi:10.1128/MCB.01421-08

The Mitogen-Activated Protein Kinase Scaffold KSR1 Is Required for Recruitment of Extracellular Signal-Regulated Kinase to the Immunological Synapse▽

Emanuele Giurisato,[1] Joseph Lin,[1] Angus Harding,[1]† Elisa Cerutti,[1] Marina Cella,[1] Robert E. Lewis,[2] Marco Colonna,[1] and Andrey S. Shaw[1,3]*

Department of Pathology & Immunology, Washington University School of Medicine, St. Louis, Missouri 63110[1]; Department of Pathology, University of Nebraska Medical Center, Eppley Cancer Institute, Omaha, Nebraska 68198-7696[2]; and Howard Hughes Medical Institute, Washington University School of Medicine, St. Louis, Missouri 63110[3]

Received 10 September 2008/Returned for modification 8 October 2008/Accepted 19 December 2008

KSR1 is a mitogen-activated protein (MAP) kinase scaffold that enhances the activation of the MAP kinase extracellular signal-regulated kinase (ERK). The function of KSR1 in NK cell function is not known. Here we show that KSR1 is required for efficient NK-mediated cytolysis and polarization of cytolytic granules. Single-cell analysis showed that ERK is activated in an all-or-none fashion in both wild-type and KSR1-deficient cells. In the absence of KSR1, however, the efficiency of ERK activation is attenuated. Imaging studies showed that KSR1 is recruited to the immunological synapse during T-cell activation and that membrane recruitment of KSR1 is required for recruitment of active ERK to the synapse.

Kinase suppressor of Ras was originally identified in *Drosophila melanogaster* (53) and *Caenorhabditis elegans* (19, 32, 52) as a positive regulator of the extracellular signal-regulated kinase (ERK) mitogen-activated protein (MAP) kinase signaling pathway. It is thought to function as a MAP kinase scaffold because it can bind to Raf, MEK, and ERK (18, 19, 27, 28, 44, 59). While the exact function of KSR is unknown, preassembling the three components of the ERK MAP kinase cascade could function to enhance the efficiency of ERK activation, potentially regulate the subcellular location of ERK activation, and promote access to specific subcellular substrates (16, 45, 46).

While only one isoform of KSR is expressed in *Drosophila* (53), two KSR isoforms have been identified in *C. elegans* (19, 32, 52) and most higher organisms. They are referred to as KSR1 and KSR2 (32, 43). While KSR1 mRNA and protein are detectable in a wide variety of cells and tissues, including brain, thymus, and muscle (10, 11, 29), little is known about the expression pattern of KSR2.

We previously reported the phenotype of KSR1-deficient mice (30). These mice are born at Mendelian ratios and develop without any obvious defects. Using gel filtration, we showed that KSR1 promotes the formation of large signaling complexes containing KSR1, Raf, MEK, and ERK (30). Using both primary T cells stimulated with antibodies to the T-cell receptor as well as fibroblasts stimulated with growth factors, we showed that KSR1-deficient cells exhibit an attenuation of ERK activation with defects in cell proliferation.

Here we explored the role of KSR1 in NK cell-mediated cytolysis. The killing of a target cell by a cytolytic T cell or NK cell is a complicated process that involves cell polarization with microtubule-dependent movement of cytolytic granules to an area that is proximal to the contact surface or immunological synapse (7, 33, 34, 48–50, 54). A variety of different signaling molecules are also involved, including calcium (23), phosphatidylinositol-3,4,5-triphosphate (13, 17), and activation of the ERK MAP kinase (6, 42, 56). Recently, the recruitment of activated ERK to the immunological synapse (IS) has been shown to be a feature of successful killing of a target by cytotoxic T lymphocytes (58).

How active ERK is recruited to the synapse is not known. Since KSR1 is known to be recruited to the plasma membrane by Ras activation (24), and since the immunological synapse is one of the major sites of Ras activation (26, 41), it seemed plausible to test the hypothesis that KSR1 recruitment to the plasma membrane functions to recruit ERK to the immunological synapse and facilitate its activation. We found that KSR1 was recruited to the immunological synapse and that KSR1 appeared to be required for the localization of active ERK at the contact site. As KSR1-deficient cells exhibit a defect in killing, this suggests that KSR1 recruitment to the synapse may be important in the cytolytic killing of target cells.

MATERIALS AND METHODS

Mice. KSR1-deficient mice (*KSR1*$^{-/-}$) have been described previously (30). All mice were housed under specific-pathogen-free conditions in the Washington University animal facilities in accordance with institutional guidelines.

Cell cultures and antibodies. Jurkat E6.1 T cells, Daudi lymphoma B cells, YAC-1 lymphoma cells, human K562 eritroblastoma cells, and RMAs and RMAs-Rae1ε cells were grown in RPMI 1640 medium supplemented with 10% fetal bovine serum (FBS). Human interleukin-2 (hIL-2)-dependent cell line NK92 cells (15) were grown in RPMI 1640 medium supplemented with 10% FBS and 100 U/ml of hIL-2. Mouse NK cells were purified by DX5^{+} magnetic-activated cell sorting enrichment (Miltenyi) and grown in hIL-2-containing medium (5). Polyclonal rabbit anti-Grb2, rabbit anti-ERK2, rabbit anti-KSR1, and mouse anti-Lck were obtained from Santa Cruz Biotechnology. Polyclonal rabbit anti-phospho-ERK [pERK1/2 (Thr202/Tyr204)] and rabbit anti-phospho-

* Corresponding author. Mailing address: Department of Pathology & Immunology, Washington University School of Medicine, St. Louis, MO 63110. Phone: (314) 362-6311. Fax: (314) 362-8888. E-mail: shaw@pathology.wustl.edu.

† Present address: Queensland Brain Institute, University of Queensland, QBI Building 79, St. Lucia, QLD 4072, Australia.

▽ Published ahead of print on 12 January 2009.

MAPK/CDK substrates (PXSP) were obtained from Cell Signaling Technology. Monoclonal anti-MAP kinase (diphosphorylated ERK1/2) and mouse anti-α-tubulin were purchased from Sigma. Fluorescein isothiocyanate-labeled CD3ε and phycoerythrin (PE)-NK1.1-labeled antibody were obtained from BD Biosciences.

Generation of DNA constructs. Murine KSR1 (mKSR1) full-length cDNA was subcloned into a pEYFP-N1 vector (Clontech). After EcoRI and NotI digestion, mKSR1-YFP was cloned into a pMX retrovirus vector (31). The C359 and C362 mutants in the CA3 domain of mKSR1 (CCSS mutant) were generated using PCR site-directed mutagenesis (Stratagene). The primers used for C359S were 5′-G ATT TTT GGC GTG AAG AGC AAA CAC TGC AGG-3′ and 5′-CCT GCA GTG TTT GCT CTT CAC GCC AAA AAT C-3′; for C362S they were 5′-GTG AAG AGC AAA CAC AGC AGG TTA AAA TGC CAT AAC-3′ and 5′-GTT ATG GCA TTT TAA CCT GCT GTG TTT GCT CTT CAC-3′. The integrity of all constructs was confirmed by automated sequencing.

Retroviral transduction. The Phoenix amphotropic retroviral packaging cell line was kindly provided by Garry Nolan. After transfection using Lipofectamine 2000 (Life Technologies), cells were transferred to 32°C to allow accumulation of virus in the supernatant. Virus-containing supernatant was harvested at 24 and 48 h after transfection and filtered through 0.45-μm syringe filters (Millipore). Jurkat cells were incubated with viral supernatant in the presence of 8 μg/ml of Polybrene (Sigma) and then centrifuged at 900 × *g*. This step was repeated after 4 h. Cells expressing yellow fluorescent protein (YFP) were sorted 3 to 5 days later on a Beckton Dickinson FACSVantage SE at the Flow Cytometry Core Facility (Dept. of Pathology and Immunology, Washington University, St. Louis, MO).

RNA interference and lentivirus production. KSR1 small hairpin RNA (shRNA) and luciferase shRNA (control) constructs were generated using the multifunctional lentivirus system (pFLRu lentivector; provided by Y. Feng and G. D. Longmore). To generate human KSR1 shRNA fragments, two sequences corresponding to nucleotides 1507 to 1530 and 2139 to 2157 were selected. Primers (sequence 1 forward, GTG GAA AGG ACG AAA CAC CGC CTA CTT CAT TCA TCA TAG ATA GCA TTC AAG AGA TGC TG; sequence 2 forward, GTG GAA AGG ACG AAA CAC CGC AGA CGT CTC TGG ACG TCA ATT CAA GAG ATT GAT GT) were designated together with their complementary counterparts and annealed by PCR to obtain shRNA fragments. Joint PCR was carried out by using human U6 promoter forward primer (ACA GAA TTC TAG AAC CCC AGT GGA AAG ACG CGC AG), shRNA reverse primer, and mixed template (1 μl of purified human U6 promoter and 2 μl of purified shRNA fragment). The PCR products were purified, digested with XhoI/XbaI, and subcloned into pFLRu lentivector [pFLRu-(KSR1-shRNA)]. To reconstitute KSR1 expression, mKSR1-YFP wild type and CCSS mutant were subcloned into the pFLRu-KSR1#1-shRNA vector to create pFLRu-(KSR1#1-shRNA)-mKSR1(WT)-YFP and pFLRu-(KSR1#1-shRNA)-mKSR1(CCSS)-YFP, respectively. The integrity of all constructs was verified by automated sequencing. For lentivirus production, subconfluent cultures of 293T cells were transfected with packaging plasmid (pHR′8.2ΔR/pCMV-VSV-G at a ratio of 8:1) and pFLRu-derived plasmid (Y. Feng, H. Zhao, B. Wang, and G. D. Longmore, submitted for publication) using Lipofectamine 2000. The lentivirus infection of Jurkat cells was performed using the protocol described above, and cells expressing the same level of YFP were sorted 3 to 5 days later.

Confocal imaging and immunofluorescence staining. To study the recruitment of phosphorylated ERK (pERK) into the immunological synapse, purified NK cells from wild-type (WT) or *KSR1*$^{-/-}$ mice were mixed with equal amount of carboxyfluorescein succinimidyl ester (CFSE)-preloaded YAC-1 target cells. After centrifugation, cells were gently resuspended and placed onto poly-D-lysine-coated glass slides for 10 min at 37°C. After aspiration of the medium, cells were fixed with 4% paraformaldehyde in phosphate-buffered saline (PBS) for 10 min. Cells were permeabilized with 90% methanol for 30 min at −20°C, washed with PBS containing 4% FBS, and incubated with mouse anti-pERK for 45 min at room temperature. After washing, cells were incubated with Cy3-conjugated anti-mouse immunoglobulin (Jackson ImmunoResearch Laboratories, Inc.) for 30 min at room temperature. To image the lytic granule polarization, the indicated mouse NK cells were loaded with 100 nM Lysotracker (Molecular Probes) for 20 min at 37°C. After washing, loaded mouse NK cells were mixed with RMAs-Rae1ε target cells at a 1:1 ratio and flowed onto a parallel plate of flow cells in a temperature-controlled chamber at 37°C. Images were taken over 0 to 20 min using a Zeiss LSM 510 laser-scanning confocal microscope (Oberkochen, Germany) with 63× objective lenses. To study the recruitment of KSR1 and pERK into the T-cell immunological synapse, transduced Jurkat cells were mixed with an equal amount of Daudi B cells preloaded with or without staphylococcal enterotoxin E (SEE). After centrifugation, cells were gently resuspended, placed onto poly-L-lysine-coated glass slides for 5 min at 37°C, fixed, permeabilized, and stained as described above. To quantitate the recruitment of KSR1-YFP or *YFP* to the contact site, boxes were drawn at the contact area between the effector and target cells, at the cytosol, and in a background area outside the cell by using the Image J software program (NIH). The relative recruitment index (RRI) was calculated as follows: (mean fluorescence intensity [MFI] at synapse − background)/(MFI at regions in the cytosol − background). For each experiment, the percentage of Jurkat cells with an RRI of more than 1.1 was calculated. For quantification of pERK translocation to the cell-cell contact area, the ratio of MFI at the contact area versus an equivalent in the cytosol was calculated and a ratio of more than 1.1 was scored as protein accumulation. At least 50 conjugates were examined for each experiment, and three different experiments were performed.

Cytotoxicity assays. Cytotoxic activity of mouse NK cells was tested against YAC-1 or RMAs or RMAs-Rae1ε target cells using standard 4-h ^{51}Cr release assays (5). Where indicated, NK cells were preincubated with 10 μM specific MEK inhibitor (UO126; Calbiochem) at 37°C for 30 min. In all experiments, spontaneous release did not exceed 10% of maximum release.

CFSE labeling and in vivo NK killing assay. The in vivo NK cell cytolytic experiments were performed essentially as previously described (3). RMAs and RMAs-Rae1ε cells (10^7) were labeled with 1 μM (low peak) and 10 μM (high peak) CFSE (Molecular Probes) for 15 min at 37°C in RPMI 1640 medium supplemented with 5% FBS. Labeling was blocked with 1:1 (vol/vol) FBS, and cells were washed several times with RPMI complete medium. CFSE-loaded cells were counted, mixed at a 1:1 ratio, and injected intraperitoneally (8×10^6 to 10×10^6 cells/mouse in a 300-μl volume) in WT and *KSR1*$^{-/-}$ mice. A small sample of injection mix was acquired at the zero time point to record the ratio between RMAs and RMAs-Rae1ε cells. At 24 h after injection, cells were recovered by peritoneal lavage. After washing, the Rae1ε expression was monitored by binding with a specific antibody (anti-Rae1ε antibody conjugated to biotin; provided by Marina Cella) followed by the appropriate secondary antibody. The ratio between RMAs and RMAs-Rae1ε cells from CFSE-labeled cells was determined by flow cytometry.

Cell conjugation assay. Target cells were loaded with 10 μM CFSE for 15 min at 37°C. NK cells from WT or *KSR1*$^{-/-}$ mice were stained with PE-labeled NK1.1 antibody (BD Biosciences). After washing, stained NK cells were mixed with CFSE-loaded target cells at a 1:1 ratio, centrifuged, and incubated for 20 min at 37°C to form conjugates. After fixation in 4% paraformaldehyde in PBS for 10 min, cells were analyzed by flow cytometry.

Flow cytometric measurement of intracellular ERK activation. T cells transduced with the indicated lentivectors were mixed with SEE-pulsed Daudi B cells at a 1:1 ratio, spun at 350 × *g* for 10 s, and placed at 37°C for 5 min. T-cell–antigen-presenting cell (APC) conjugates were then separated with ice-cold PBS–2.5 mM EDTA and fixed with 4% paraformaldehyde for 10 min on ice. Cells were permeabilized with 90% methanol for 30 min at −20°C, washed with PBS containing 3% fetal bovine serum, and incubated with mouse anti-pERK for 45 min at room temperature. After washing, cells were incubated with phycoerythrin-labeled F(ab′)$_2$ anti-mouse immunoglobulin (Jackson ImmunoResearch Laboratories, Inc.) for 30 min at room temperature. Staining was measured by flow cytometry after gating for YFP-positive T cells and analyzed using FlowJo.

Cell stimulation, immunoprecipitation, and immunoblotting. Jurkat cells transduced with the indicated lentivectors were starved for 1 h in RPMI 1640. Daudi cells were loaded with 100 ng/ml of SEE (Toxin Technology, Inc.) for 30 min before mixing 2:1 (T cells:B cells) with T cells in RPMI medium. Cells were gently centrifuged for 30 s and placed at 37°C for the indicated times. After stimulation, the pellet was resuspended in ice-cold lysis buffer (0.1 M Tris base, 140 mM NaCl, 1 mM EDTA, 1% NP-40, 1 mg/ml apoprotein, 1 mM phenylmethylsulfonyl fluoride, 1 mM sodium orthovanadate, and 50 mM sodium fluoride). After centrifugation, proteins from cell lysates were resolved by sodium dodecyl sulfate-polyacrylamide gel electrophoresis (SDS-PAGE) and analyzed by immunoblotting with the indicated primary antibodies followed by incubation with anti-mouse immunoglobulin G or anti-rabbit immunoglobulin G coupled to horseradish peroxidase. To quantified the level of KSR1, whole-cell lysates from Jurkat or NK92 cells transduced with the indicated lentivector were resolved by SDS-PAGE. KSR1 protein bands were detected and quantified by immunoblotting with the Odyssey system (Li-Cor). NK92 cells (5×10^6/sample) transduced with the indicated lentivectors, after sorting, were IL-2 starved for 4 h in RPMI 1640 containing 5% FBS. Cells were incubated with an equal number of K562 target cells at 37°C for the indicated times. Cells were resuspended in ice-cold lysis buffer and were centrifuged as described above. Cell lysates were analyzed by immunoblotting with antibodies specific for phosphorylated ERK. In the immunoprecipitation experiments, nucleus-free supernatant was incubated with 2 μg/ml of monoclonal anti-Lck at 4°C for 60 min and then incubated with protein A-Sepharose beads (Pharmacia) at 4°C for 90 min. After washing, Lck

immunoprecipitates were resolved by SDS-PAGE, transferred to a membrane, and analyzed by immunoblotting with the indicated antibodies.

Statistics. Statistical analyses were performed using a paired Student's *t* test. Differences that were statistically significant are noted in the figures below.

RESULTS

KSR1 is required for NK lytic activity. Previously we showed that thymic and peripheral T-cell populations in *KSR1*$^{-/-}$ mice were similar to wild type (30). To determine the role of KSR1 in NK cell development, we measured the numbers of NK cells by using antibodies to CD3 and NK1.1 in the spleens of wild-type and *KSR1*$^{-/-}$ mice (Fig. 1A). Flow cytometric analysis showed that NK cells (NK1.1$^+$ CD3$^-$ cells) were normally represented in spleens of *KSR1*$^{-/-}$ mice (Fig. 1B). We also observed that KSR1 deficiency did not affect the numbers of NKT cells (NK1.1$^+$ CD3$^+$). Altogether, these data suggest that NK cell development is normal in *KSR1*$^{-/-}$ mice.

We then tested the role of KSR1 in NK cell killing. Splenic NK cells from wild-type and KSR1-deficient mice were purified and NK lytic activity was tested by incubation with YAC-1 target cells. While wild-type NK cells efficiently killed YAC-1 cells (Fig. 2A), there was a significant reduction of killing when using KSR1-deficient NK cells.

Since YAC-1 cell recognition is complex and involves several different receptors (5), we also tested NK lytic activity mediated by the NK receptor NKG2D. For these experiments we used RMAs cells transfected with the mouse NKG2D ligand Rae1ε (RMAs-Rae1ε) as targets. NK cells from KSR1-deficient mice showed a significant reduction in cytolytic activity (Fig. 2B) that was specific to NKG2D, as there was no killing of RMAs cells lacking Rae1ε expression. Importantly, the reduction of NK cell cytotoxicity was not mediated by the decreased cell-cell adhesion, since the absence of KSR1 did not affect the ability of NK cells to form conjugates with the indicated target cells (Fig. 2C).

We confirmed the NK cell killing defect in vivo by injecting wild-type and KSR1-deficient mice with RMAs and RMAs-Rae1ε cells and monitoring tumor growth as previously described (3). In this system, elimination of RMAs-Rae1ε cells is mediated by NK cells in an NKG2D-dependent manner. RMAs and RMAs-Rae1ε cells (10^7) were distinguished by labeling with either 1 μM (low staining) or 10 μM (high staining) CFSE, respectively. Tumor cells were mixed at a 1:1 ratio and injected intraperitoneally (8×10^6 to 10×10^6 cells/mouse in a 300-μl volume). A sample was measured before injection to document the starting ratio between RMAs and RMAs-Rae1ε cells (Fig. 2D and G). Twenty-four hours after injection, cells were recovered by peritoneal lavage and stained with anti-Rae1ε, and the ratio between RMAs and RMAs-Rae1ε cells in the CFSE-labeled cells was determined by flow cytometry. As expected (12), RMAs-Rae1ε cells were preferentially eliminated in wild-type mice (Fig. 2E and G). In contrast, elimination of RMAs-Rae1ε cells in *KSR1*$^{-/-}$ mice was impaired (Fig. 2F and G). This demonstrates that KSR1 is required to mediate NK cell lytic activity in vivo.

NKG2D-induced lytic granule polarization is impaired in *KSR1*$^{-/-}$ mice. NK killing of the target cells is mediated by the polarized release of lytic granules (13, 34). Since NK lytic activity was impaired in the absence of KSR1, we investigated whether KSR1 was required for lytic granule polarization. Purified NK cells from wild-type and *KSR1*$^{-/-}$ mice were incubated with Lysotracker to label lytic granules and then imaged before and after conjugate formation with YAC-1 cells. Prior to conjugation, lytic granules were randomly distributed in the cytosol (Fig. 3A). After interaction with YAC-1 cells, lytic granules of wild-type NK cells moved to a location near the site of contact with the target cell (Fig. 3A and C). This was spe-

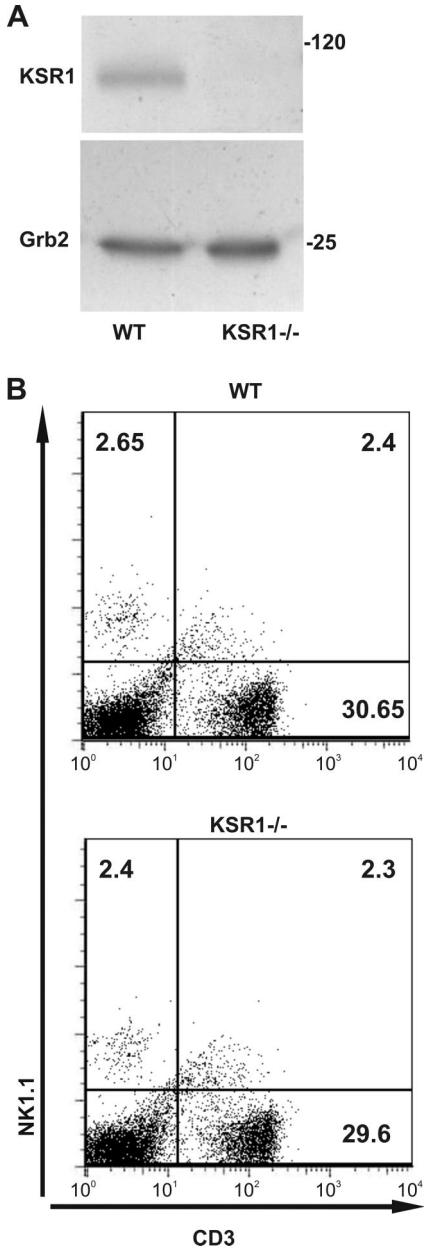

FIG. 1. Normal numbers of NK cells in *KSR1*$^{-/-}$ mice. (A) Expression of KSR1 in splenocytes of WT and *KSR1*$^{-/-}$ mice. Total cell lysates of WT and *KSR1*$^{-/-}$ mice were analyzed by immunoblotting with anti-KSR1 antibody. Grb2 antibody was used as a loading control. (B) Splenocytes of WT and *KSR1*$^{-/-}$ mice were stained with NK1.1-PE and CD3ε-fluorescein isothiocyanate antibody and analyzed by flow cytometry. The dot blot is representative of three different experiments (two mice/experiment).

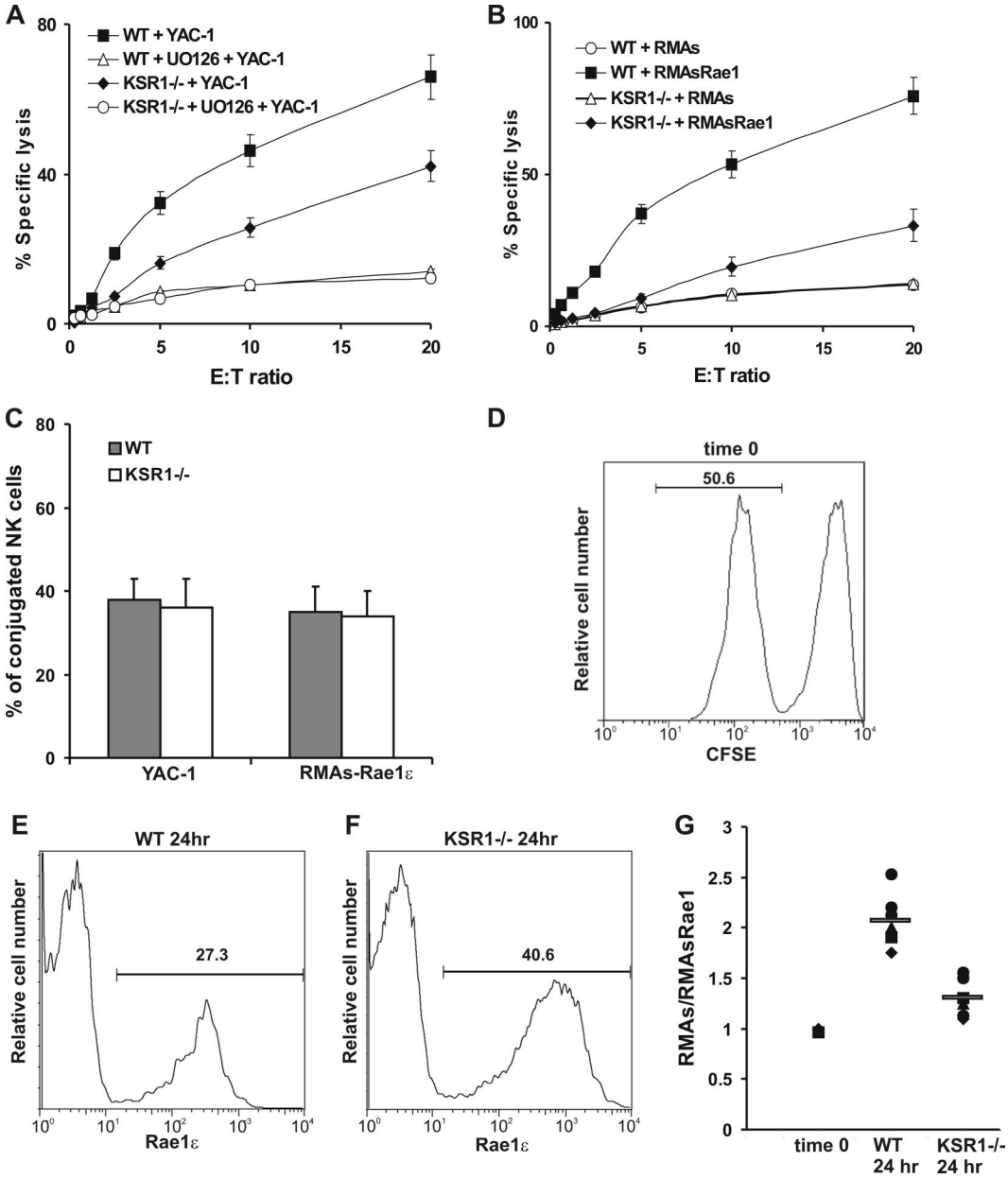

FIG. 2. KSR1 is required for NK lytic activity in vitro and in vivo. (A and B) Cytotoxicity of WT and *KSR1*$^{-/-}$ NK cells was tested against YAC-1 cells (A) or RMAs and RMAs-Rae1ε target cells (B) in vitro. Purified NK cells (>96% NK1.1$^+$ CD3ε$^-$) were IL-2 starved in RPMI medium for 4 h before incubation with the indicated target cells. Where indicated, NK cells were preincubated with the MEK inhibitor UO126 (10 μM). Data are representative of three independent experiments. E:T ratio, effector:target ratio. (C) Conjugate formation is normal in KSR1-deficient cells. NK cells from WT or *KSR1*$^{-/-}$ mice were stained with NK1.1-PE antibody and mixed with CFSE-loaded target cells. Cells were allowed to form conjugates for 20 min at 37°C, fixed, and analyzed by flow cytometry. The bar graphs represent the percentages of NK1.1$^+$ CFSE$^+$ double-positive cells from the total pool of NK1.1$^+$ cells. Data are represented as averages ± standard errors of the means of at least three separate experiments. (D to G) NK killing assay in vivo. RMAs and RMAs-Rae1ε cells were labeled with different concentrations of CFSE and mixed at a 1:1 ratio. (D) An aliquot of the cell mixture was analyzed before injection (time zero). (E and F) The cell mixture was injected intraperitoneally into WT and *KSR1*$^{-/-}$ mice. Twenty-four hours after injection, cells were recovered by peritoneal lavage. Rae1ε expression was assessed by labeling with anti-Rae1ε antibody and examined by flow cytometry. The RMAs/RMAs-Rae1ε ratio was obtained by comparing high and low CFSE-labeled cells. (G) Summary of RMAs/RMAs-Rae1ε ratios in six WT and six *KSR1*$^{-/-}$ mice. Horizontal bars indicate the mean ratios.

cific, as the polarized movement of lytic granules was inhibited by using inhibitors of phosphatidylinositol 3 kinase (data not shown). While the ability of KSR1-deficient NK cells to form conjugates with YAC-1 cells was not affected, lytic granule polarization was significantly reduced (Fig. 3B and C). These results suggest that KSR1 is also important in lytic granule polarization and that defects in granule polarization may be responsible for defects in cytolytic killing.

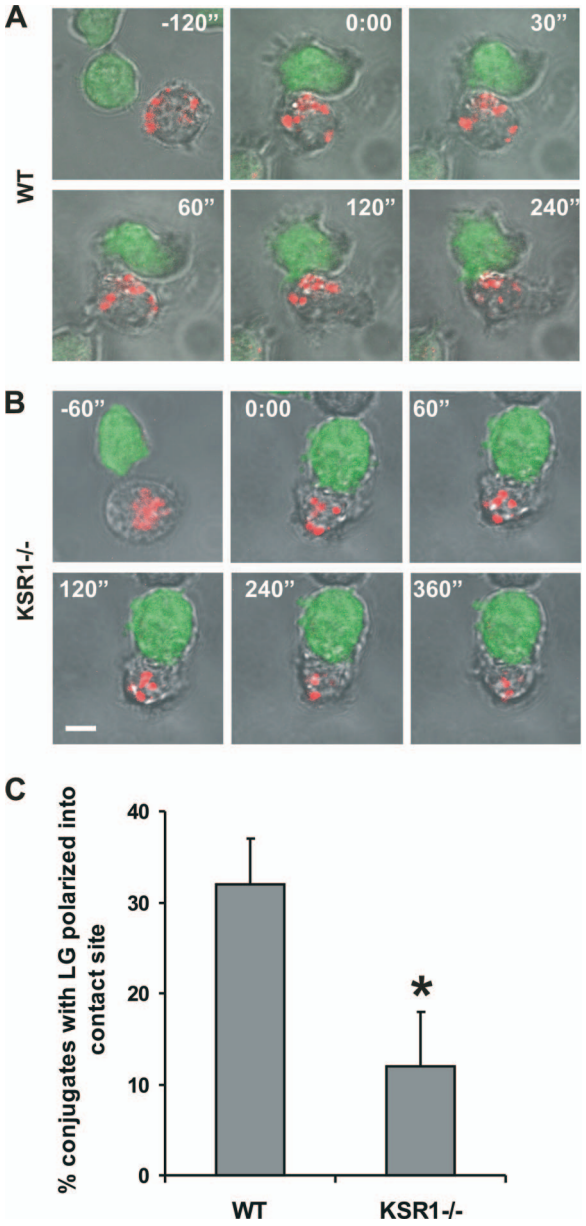

FIG. 3. Lytic granule polarization is impaired in NK cells from *KSR1*$^{-/-}$ mice. (A and B) Time-lapse experiment, extracted from a movie, showing representative images of the localization of lytic granules (red) in primary NK cells purified from spleens of WT (A) and *KSR1*$^{-/-}$ (B) mice and conjugated with CFSE-loaded YAC-1 target cells (green; time in seconds). Bar, 5 μm. (C) Lytic granule (LG) polarization at the contact site with the indicated target cells was quantitated after 5 min of incubation. Data represent the mean (±standard error of the mean) percentage of conjugates from three independent experiments with at least 40 conjugates. *, $P < 0.05$.

pERK recruitment into the NK IS is impaired in *KSR1*$^{-/-}$ mice. Recently it has been reported that pERK is recruited to the immunological synapse of CD8$^+$ T cells (58). Since it is postulated that the subcellular localization of signaling molecules is mediated by scaffold molecules (18, 39, 45), we wondered whether KSR1 might be involved in ERK localization to the IS.

We tested whether KSR1 plays a role in pERK localization by first imaging pERK localization using NK cells from KSR1-deficient mice. Purified NK cells from wild-type and *KSR1*$^{-/-}$ mice were conjugated with YAC-1 cells. Cells were stained with antibodies to pERK and analyzed by confocal microscopy. While pERK was detectable in both wild-type and KSR1-deficient NK cells, pERK localization at the synapses was infrequent in KSR1-deficient NK cells compared to wild-type cells (Fig. 4A and B).

So that we could dissect the mechanism of KSR1 function, we attempted to replicate these findings using Jurkat cells where KSR1 expression was suppressed using lentiviruses expressing two different KSR1-specific shRNAs. Bulk sorting of green fluorescent protein-positive cells showed that both shRNAs resulted in over 70% inhibition of expression (Fig. 4C). pERK recruitment to the synapse was then analyzed by forming conjugates between Jurkat cells and superantigen-coated APCs (Fig. 4D and E). While pERK was easily detected at the IS of conjugates formed using wild-type Jurkat cells (Fig. 4D, upper panels, and E), suppression of KSR1 expression significantly impaired the recruitment of pERK to the IS (Fig. 4D, lower panels, and E). Similar results were obtained when the same shRNAs were used in the human NK cell line NK92 (data not shown).

Consistent with results from KSR-deficient T cells (30), suppression of KSR1 expression in the Jurkat cells attenuated ERK activation (Fig. 5A). This suggested that our inability to detect pERK at the synapse could be due to a generalized defect in ERK activation. This seemed unlikely, as strong staining with the pERK antibody was easily detected in some of the KSR1-deficient cells (Fig. 4D). Germain and coworkers have demonstrated that ERK activation by the T-cell receptor is all or none in individual CD8$^+$ T cells (1). What they found was as the strength of T-cell receptor (TCR) signaling increases, there is not a graded increase in ERK activation. Rather, at the individual cell level, ERK is either fully activated in cells or not activated at all. We, therefore, hypothesized that in the absence of KSR1, cells could still be activated but that the total number of activated cells was lower. To confirm this, we used flow cytometry to compare ERK activation in control versus KSR1 shRNA-treated cells. As we expected, KSR1 shRNA cells were able to activate ERK to levels similar to wild-type cells but the number of cells that were activated was much lower (Fig. 5B). This suggests that KSR1 functions to increase the sensitivity of TCR-mediated activation of ERK. In addition, it suggests that the lack of pERK at the synapse is not due to a generalized defect in ERK activation and supports the hypothesis that KSR1 is required for the synapse localization of pERK.

KSR1 recruitment is required for pERK accumulation into the immunological synapse. To determine whether KSR1 itself is recruited to the IS, Jurkat T cells were transduced with a construct encoding KSR1 fused to YFP (KSR1-YFP). After conjugation with superantigen-coated APCs, KSR1-YFP was easily detected at the IS (Fig. 6A, lower panel, and B). As a control, YFP by itself was distributed homogenously throughout Jurkat cells with or without stimulation by SEE (Fig. 6C). The KSR1-YFP recruitment was specific to T-cell activation, as conjugation with APCs in the absence of superantigen did

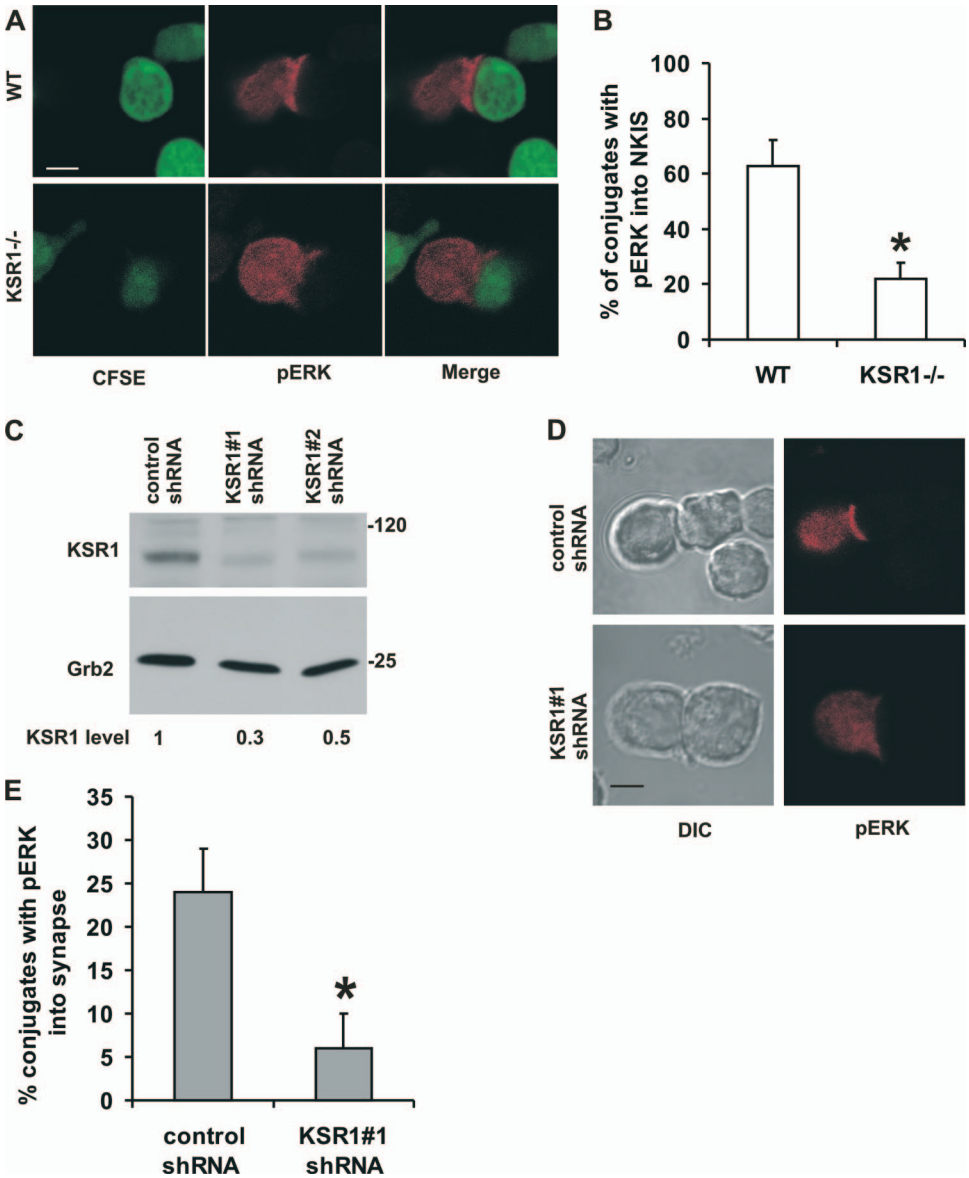

FIG. 4. Recruitment of pERK into the NK IS is impaired in KSR1-deficient mice. (A) Representative images showing the localization of pERK (red) in primary NK cells purified from spleens of WT and *KSR1*$^{-/-}$ mice that were conjugated with CFSE-loaded YAC-1 target cells (green). Bar, 5 μm. (B) pERK accumulation at the NK IS was quantitated by dividing the percentage of cells with pERK at the NK IS by the total number of pERK-positive cells imaged. Data represent the mean (±standard error of the mean) percentage of conjugates with an RRI (see Materials and Methods) of >1.1, from three independent experiments with at least 30 conjugates. *, $P < 0.05$. (C) KSR1 knockdown in Jurkat T cells. Immunoblotting results are for KSR1 and Grb2 expression in Jurkat T cells (3.5×10^6 cells/lane) transduced with the indicated shRNA. KSR1 expression levels were compared to control shRNA Jurkat T cells. (D) pERK recruitment into the contact site is impaired in KSR1 knockdown T cells. Representative differential interference contrast and Cy3 fluorescence images are shown for shRNA-expressing Jurkat T cells conjugated with Daudi B cells preloaded with 100 ng/ml of superantigen. Bar, 5 μm. (E) Percentage of conjugates with pERK recruited into the synapse, as described for panel D. Quantitative analysis was done for pERK accumulation at the contact site from three independent experiments with at least 40 conjugates. Data represent the mean (±standard error of the mean) percentage of conjugates with an RRI of >1.1. *, $P < 0.05$.

not result in any detectable KSR1 recruitment to the synapse (Fig. 6A, upper panel, and B).

After Ras activation, KSR1 is recruited to the plasma membrane via its CA3 domain (24). To verify that synapse recruitment of KSR1 is responsible for pERK localization in the synapse, we rescued KSR1-deficient Jurkat cells with either a CA3-mutated KSR1-YFP construct or a wild-type KSR1-YFP fusion. The CA3 domain has two conserved cysteine residues that can be mutated to disrupt the structure of the domain and its ability to bind to membranes (60). Cell sorting was used to isolate a population of cells with similar expression levels (Fig. 7A). Since high-level expression of KSR1 is known to inhibit ERK activation (20, 21), we first verified that the level of KSR1 expression in the cells that we isolated was able to restore ERK activation. Flow cytometric analysis showed that the level of wild-type KSR1 was sufficient to reconstitute ERK activation.

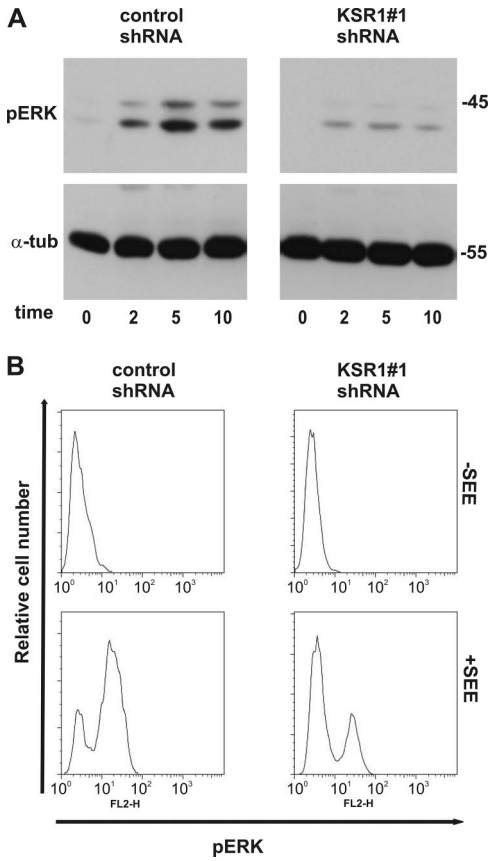

FIG. 5. Antigen-induced T-cell activation is regulated by KSR1. (A) ERK activation is impaired in KSR1 knockdown T cells. shRNA-transduced Jurkat T cells were stimulated with superantigen-coated Daudi cells (100 ng/ml) for the indicated times (in minutes) and analyzed for pERK1/2 by Western blotting. Blotting for α-tubulin (α-tub) was used to demonstrate equal loading of each sample. (B) Suppression of KSR1 expression inhibits the number of activated Jurkat cells. Representative histograms show the distribution of pERK as measured by flow cytometry of Jurkat T cells after activation by Daudi preloaded with or without superantigen (10 ng/ml SEE). In the absence of stimulation, no shift in the *x* axis of histograms was observed in either control or KSR1 shRNA-expressing Jurkat cells. Notably, after stimulation the change in area under the peak indicates that ERK activation was observed in a higher number of control shRNA cells.

Interestingly, the CA3 mutant was able to partially rescue ERK activation, suggesting that KSR1 can facilitate ERK activation in the absence of membrane recruitment (Fig. 7B).

We next tested whether cells expressing the CA3-mutated KSR1-YFP could rescue pERK localization at the IS. Imaging experiments showed that the wild-type KSR1-YFP was recruited to the synapse and was able to rescue pERK localization at the IS. In contrast, the CA3 mutant was not recruited to the IS, nor was pERK detectable at the IS (Fig. 7C and D). Together, these results demonstrate that KSR1 recruitment to the IS is mediated by its CA3 domain and that KSR1 recruitment to the IS is required for pERK localization at the immunological synapse.

Phosphorylation of the Lck PXSP motif is regulated by KSR1-mediated ERK activation. The requirement for active ERK recruitment to the IS suggests that it is required for the phosphorylation of proteins that are present in the synapse. Since Lck is a known substrate for ERK during T-cell activation (47, 55, 57), we tested whether KSR1 was required for Lck phosphorylation. A KSR1-specific shRNA-expressing lentivirus was used to inhibit endogenous KSR1 expression in a human NK cell line (Fig. 8A). We confirmed that suppression of KSR1 reduced ERK activation in the human NK cell line after stimulation with target cells (K562 cells) (Fig. 8B). Lck immunoprecipitates were prepared from both wild-type and KSR1 shRNA-expressing cells and blotted with an antibody that recognizes ERK phosphorylation sites (PXSP). The induction of Lck phosphorylation after target cell incubation was reduced in KSR1 shRNA-treated NK cells compared to wild-type cells (Fig. 8C). This supports the hypothesis that KSR1 recruitment of ERK facilitates the phosphorylation of ERK substrates at the synapse.

DISCUSSION

Here we examined the role of KSR1 on the cytolytic function of NK cells and found that KSR1-deficient NK cells exhibit a defect in killing. The defect appeared to be related to an inability to polarize cytolytic granules. Since pERK recruitment to the immunological synapse was recently reported during the activation of $CD8^+$ T cells (58), and because ERK activation is required for killing (6, 56), we explored the hypothesis that pERK recruitment to the synapse might be facilitated by KSR1. Indeed, we found that in KSR1-deficient T cells, pERK recruitment to the immunological synapse was defective.

KSR1 is thought to function as a scaffold for the Ras/MAP kinase pathway (18, 27, 28, 44). This scaffold molecule regulates the intensity and duration of growth factor-induced ERK activation to modulate a cell's proliferative, oncogenic, and adipogenic potential (20, 21, 40). It binds to all three kinases of the ERK MAP kinase cascade, Raf-1, MEK, and ERK (19, 51, 53), and is recruited to the plasma membrane during Ras activation, where it presumably facilitates the interaction between active Ras and Raf-1 (18, 28, 35). More recent data suggest that KSR may have additional roles facilitating phosphorylation of the activation loop of Raf (9). Previously, we showed that in KSR1-deficient T cells the activation of ERK was still detectable but highly attenuated (30). We interpreted this to mean that KSR1 is required for the efficient activation of ERK.

In this study, we analyzed the ERK activation defect in more detail. We previously used immunoblotting to measure ERK activation (10, 30). This method, because it relies on the lysis of millions of cells, averages the biochemical changes that occur at a specific moment in time. Using such a method, an attenuation of ERK activation could be due to attenuation of ERK activation in all cells or reflect a defect in ERK activation in some but not others. Using flow cytometry to analyze ERK activation at a single-cell level, we were surprised to find that in KSR1-deficient cells, the defect of ERK activation only affected some but not all cells. A small fraction of KSR1-deficient cells showed levels of ERK activation that are similar to wild-type cells.

Previous work had suggested that ERK activation in $CD8^+$ T cells is stochastic, that it is an all-or-none process (1). A weak stimulus results in only a few cells that are fully activated and

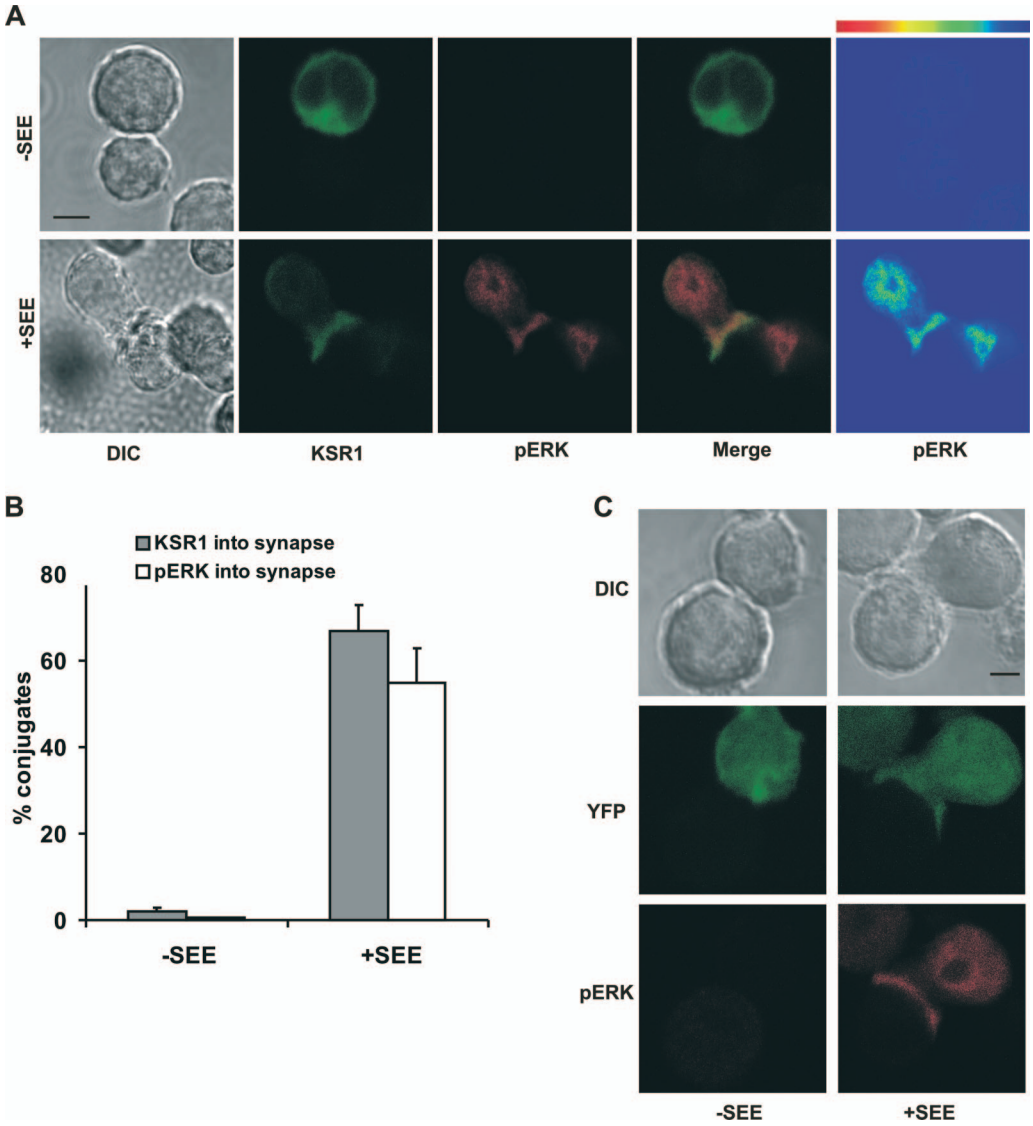

FIG. 6. KSR1 is recruited into the immunological synapse. (A) Representative differential interference contrast, YFP, and Cy3 fluorescence images of Jurkat T cells expressing KSR1-YFP after conjugation with Daudi B cells loaded with or without SEE (100 ng/ml). In the absence of SEE (-SEE), ERK (red) is not phosphorylated and KSR1 (green) is not recruited into the contact site. In the far right panel, the location of pERK is shown in false color. Bar, 5 μm. (B) KSR1 and pERK accumulation at the contact site was quantitated from three independent experiments with at least 50 conjugates. Data are represented as the average (±standard error of the mean) of conjugates with an RRI of >1.1 (see Materials and Methods). (C) Representative differential interference contrast, YFP, and Cy3 fluorescence images of Jurkat T cells expressing YFP conjugated with Daudi B cells and stimulated as for panel A. Images are representative of two independent experiments with at least 30 conjugates.

as the strength of a stimulus is increased, more and more cells show full ERK activation. In support of this idea, we found that the attenuation of ERK activation seen in KSR1-deficient cells is due to decreased numbers of activated cells, suggesting that KSR1 functions by lowering the threshold stimulus required for the stochastic activation of ERK. We speculate that by helping to recruit the Raf/MEK/ERK module to active Ras, KSR1 may function to enhance the activation of the pathway (22).

It is intriguing to speculate that recruitment of KSR1 and the ERK MAP kinase cascade to the immunological synapse may have functions in addition to simply facilitating ERK activation. By holding active ERK at the immunological synapse, KSR1 may function to allow ERK to phosphorylate specific substrates at the plasma membrane essential for T-cell function. For example, it has been proposed that ERK phosphorylation of Lck may play an important role in facilitating a positive feedback loop that is important for enhancing T-cell activation (47). Our immunoprecipitation data indicated that ERK-dependent phosphorylation of the PXSP motif in Lck was diminished after KSR1 suppression, supporting the role of KSR1 on ERK substrate phosphorylation into the synapse. Other important substrates at the immunological synapse include stathmin, a molecule that plays a key role in helping to regulate microtubule polymerization (4). It seems possible that the granule polarization defect seen in the KSR1-deficient cells

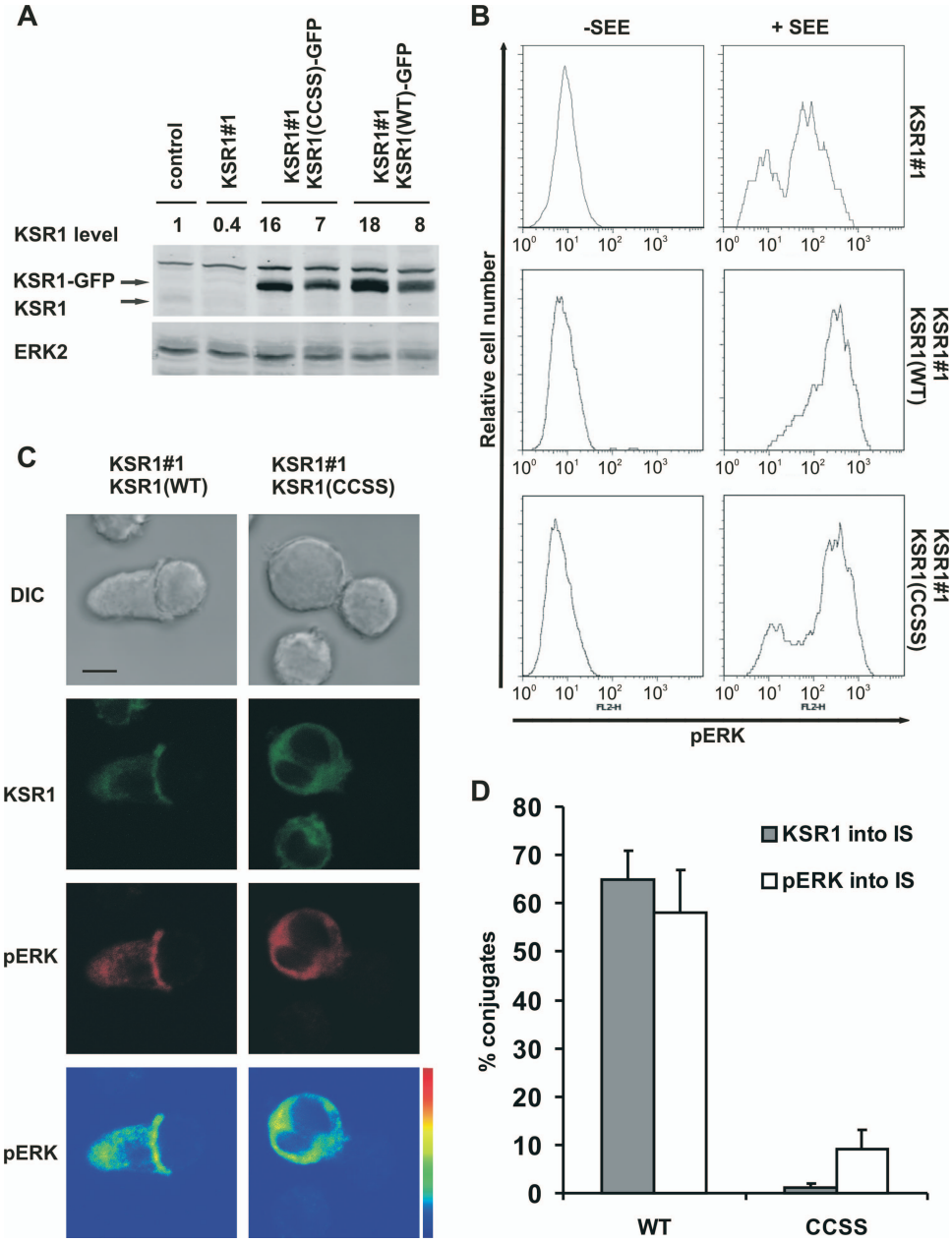

FIG. 7. KSR1 recruitment affected pERK accumulation into the contact site and antigen-induced T-cell activation. (A) Immunoblotting for KSR1 expression in Jurkat T cells (600×10^3 cells/lane) transduced with control shRNA, KSR1#1 shRNA, or rescue KSR1#1 shRNA lentivector containing KSR1(CCSS)-YFP or KSR1(WT)-YFP. Transduced Jurkat T cells with rescued CCSS mutant and WT KSR1 were sorted to achieve a pool of cells with similar expression levels (low and high) of KSR1-YFP. The KSR1 expression level compared to control shRNA transduced Jurkat T cells is indicated. (B) Representative histograms of the distribution of pERK as measured by flow cytometry of the indicated transduced Jurkat T cells after activation by Daudi cells preloaded without (-SEE) or with 1,000 ng/ml of superantigen (+SEE). (C) KSR1 is required for pERK recruitment into the IS. Images shown are representative of differential interference contrast (DIC), YFP (KSR1), and Cy3 (pERK) fluorescence images of KSR1#1 shRNA-KSR1(WT)-YFP or KSR1#1 shRNA-KSR1(CCSS)-YFP Jurkat T cells conjugated with Daudi B cells preloaded with SEE (100 ng/ml). In the far right panel, the location of pERK is shown in false color. Bar, 5 μm. (D) Quantitative analysis of KSR1 and pERK accumulation levels at the contact site from three independent experiments with at least 40 conjugates. Data are presented as the average (±standard error of the mean) of conjugates with an RRI (see Materials and Methods) of >1.1.

is due to defects in ERK phosphorylation of critical substrates at the immunological synapse.

The localization of the MAP kinase cascade at different sites in the cell has been suggested to play an important role in T-cell biology (26). While it was originally thought that Ras activation of the MAP kinase cascade could only be initiated at the plasma membrane, it has now become clear that different Ras isoforms are localized and activated at distinct intracellular membranes (2, 8, 37). At steady state, while K-Ras is mainly localized to the plasma membrane and N-Ras and H-Ras are

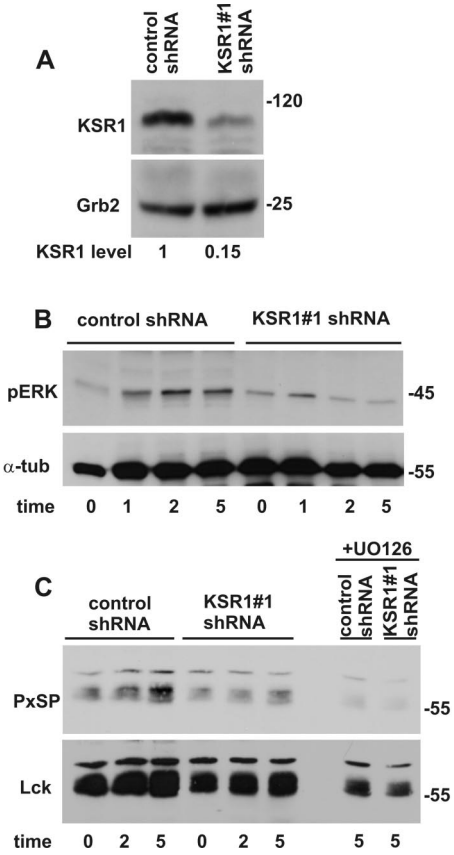

FIG. 8. ERK phosphorylation of Lck is facilitated by KSR1 in NK cells. (A) Inhibition of KSR1 expression after KSR1-specific shRNA transduction in the human NK92 cell line (3×10^6 cells/lane). Immunoblotting was performed with antibodies to KSR1 and Grb2. (B) Defective ERK activation in KSR1 knockdown NK92 cells. NK92 cells were stimulated with target cells (K562) for the indicated times (in minutes) and analyzed for pERK1/2 by Western blotting. Blotting with α-tubulin (α-tub) was used to demonstrate equal loading. (C) Serine phosphorylation of the Lck PXSP motif is facilitated by KSR1. Control and KSR1 shRNA-expressing NK92 cells were incubated with K562 cells as described for panel B. Lck immunoprecipitates were prepared at the indicated times (in minutes) and were resolved by sodium dodecyl sulfate-polyacrylamide gel electrophoresis and probed with a phospho-specific antibody to the sequence PXpSP. The membrane was then stripped and reprobed with monoclonal anti-Lck to confirm equal loading of Lck.

mainly localized to the Golgi apparatus (36). Philips and coworkers showed that TCR stimulation alone resulted mainly in Golgi complex activation of Ras, while costimulation with anti-LFA-1 allowed for plasma membrane and Golgi complex activation (25). In other systems, Ras signaling has been shown to occur on endosomes as well as in endoplasmic reticulum membranes (14, 38). Inherent in these studies is the idea that localized Ras signaling is important in the activation of location-specific effectors, but it is also possible that this plays a role in localizing active ERK close to the location-specific substrates. Unfortunately, in these studies, the localization of active ERK was not determined.

Whether KSR1 localizes to sites other than the plasma membrane is not yet known. It would be interesting if KSR1 and KSR2 were recruited to distinct membranes. Unfortunately, little is known about the expression pattern of KSR2. Probe sets for KSR2 are available on commercial microarrays for both human and mouse, but there are no data documenting any level of expression in any tissue. In our own hands, we have been unable to detect KSR2 message using a variety of different methods in any lymphoid or myeloid compartment.

ACKNOWLEDGMENTS

We thank G. Longmore and Y. Feng for providing reagents. We are grateful to Angela Fusello and Erin Filbert for helping with KSR1-deficient mice. We thank Aleksey Karpitskiy for technical assistance.

REFERENCES

1. **Altan-Bonnet, G., and R. N. Germain.** 2005. Modeling T cell antigen discrimination based on feedback control of digital ERK responses. PLoS Biol. **3:**e356.
2. **Apolloni, A., I. A. Prior, M. Lindsay, R. G. Parton, and J. F. Hancock.** 2000. H-ras but not K-ras traffics to the plasma membrane through the exocytic pathway. Mol. Cell. Biol. **20:**2475–2487.
3. **Boles, K. S., W. Barchet, T. Diacovo, M. Cella, and M. Colonna.** 2005. The tumor suppressor TSLC1/NECL-2 triggers NK-cell and $CD8^+$ T-cell responses through the cell-surface receptor CRTAM. Blood **106:**779–786.
4. **Budhachandra, K., R. K. Brojen Singh, and G. I. Menon.** 2008. Microtubule dynamics regulated by stathmin. Comput. Biol. Chem. **32:**141–144.
5. **Cella, M., K. Fujikawa, I. Tassi, S. Kim, K. Latinis, S. Nishi, W. Yokoyama, M. Colonna, and W. Swat.** 2004. Differential requirements for Vav proteins in DAP10- and ITAM-mediated NK cell cytotoxicity. J. Exp. Med. **200:**817–823.
6. **Chen, X., D. S. Allan, K. Krzewski, B. Ge, H. Kopcow, and J. L. Strominger.** 2006. CD28-stimulated ERK2 phosphorylation is required for polarization of the microtubule organizing center and granules in YTS NK cells. Proc. Natl. Acad. Sci. USA **103:**10346–10351.
7. **Chen, X., P. P. Trivedi, B. Ge, K. Krzewski, and J. L. Strominger.** 2007. Many NK cell receptors activate ERK2 and JNK1 to trigger microtubule organizing center and granule polarization and cytotoxicity. Proc. Natl. Acad. Sci. USA **104:**6329–6334.
8. **Choy, E., V. K. Chiu, J. Silletti, M. Feoktistov, T. Morimoto, D. Michaelson, I. E. Ivanov, and M. R. Philips.** 1999. Endomembrane trafficking of ras: the CAAX motif targets proteins to the ER and Golgi. Cell **98:**69–80.
9. **Douziech, M., M. Sahmi, G. Laberge, and M. Therrien.** 2006. A KSR/CNK complex mediated by HYP, a novel SAM domain-containing protein, regulates RAS-dependent RAF activation in Drosophila. Genes Dev. **20:**807–819.
10. **Fusello, A. M., L. Mandik-Nayak, F. Shih, R. E. Lewis, P. M. Allen, and A. S. Shaw.** 2006. The MAPK scaffold kinase suppressor of Ras is involved in ERK activation by stress and proinflammatory cytokines and induction of arthritis. J. Immunol. **177:**6152–6158.
11. **Giblett, S. M., D. J. Lloyd, Y. Light, R. Marais, and C. A. Pritchard.** 2002. Expression of kinase suppressor of Ras in the normal adult and embryonic mouse. Cell Growth Differ. **13:**307–313.
12. **Gilfillan, S., E. L. Ho, M. Cella, W. M. Yokoyama, and M. Colonna.** 2002. NKG2D recruits two distinct adapters to trigger NK cell activation and costimulation. Nat. Immunol. **3:**1150–1155.
13. **Giurisato, E., M. Cella, T. Takai, T. Kurosaki, Y. Feng, G. D. Longmore, M. Colonna, and A. S. Shaw.** 2007. Phosphatidylinositol 3-kinase activation is required to form the NKG2D immunological synapse. Mol. Cell. Biol. **27:**8583–8599.
14. **Gomez, G. A., and J. L. Daniotti.** 2005. H-Ras dynamically interacts with recycling endosomes in CHO-K1 cells: involvement of Rab5 and Rab11 in the trafficking of H-Ras to this pericentriolar endocytic compartment. J. Biol. Chem. **280:**34997–35010.
15. **Gong, J. H., G. Maki, and H. G. Klingemann.** 1994. Characterization of a human cell line (NK-92) with phenotypical and functional characteristics of activated natural killer cells. Leukemia **8:**652–658.
16. **Harding, A., T. Tian, E. Westbury, E. Frische, and J. F. Hancock.** 2005. Subcellular localization determines MAP kinase signal output. Curr. Biol. **15:**869–873.
17. **Jiang, K., B. Zhong, D. L. Gilvary, B. C. Corliss, E. Hong-Geller, S. Wei, and J. Y. Djeu.** 2000. Pivotal role of phosphoinositide-3 kinase in regulation of cytotoxicity in natural killer cells. Nat. Immunol. **1:**419–425.
18. **Kolch, W.** 2005. Coordinating ERK/MAPK signalling through scaffolds and inhibitors. Nat. Rev. Mol. Cell Biol. **6:**827–837.
19. **Kornfeld, K., D. B. Hom, and H. R. Horvitz.** 1995. The ksr-1 gene encodes a novel protein kinase involved in Ras-mediated signaling in C. elegans. Cell **83:**903–913.
20. **Kortum, R. L., D. L. Costanzo, J. Haferbier, S. J. Schreiner, G. L. Razidlo, M. H. Wu, D. J. Volle, T. Mori, H. Sakaue, N. V. Chaika, O. V. Chaika, and R. E. Lewis.** 2005. The molecular scaffold kinase suppressor of Ras 1 (KSR1) regulates adipogenesis. Mol. Cell. Biol. **25:**7592–7604.

21. **Kortum, R. L., and R. E. Lewis.** 2004. The molecular scaffold KSR1 regulates the proliferative and oncogenic potential of cells. Mol. Cell. Biol. **24:**4407–4416.
22. **Locasale, J. W., A. S. Shaw, and A. K. Chakraborty.** 2007. Scaffold proteins confer diverse regulatory properties to protein kinase cascades. Proc. Natl. Acad. Sci. USA **104:**13307–13312.
23. **Lyubchenko, T. A., G. A. Wurth, and A. Zweifach.** 2001. Role of calcium influx in cytotoxic T lymphocyte lytic granule exocytosis during target cell killing. Immunity **15:**847–859.
24. **Michaud, N. R., M. Therrien, A. Cacace, L. C. Edsall, S. Spiegel, G. M. Rubin, and D. K. Morrison.** 1997. KSR stimulates Raf-1 activity in a kinase-independent manner. Proc. Natl. Acad. Sci. USA **94:**12792–12796.
25. **Mor, A., G. Campi, G. Du, Y. Zheng, D. A. Foster, M. L. Dustin, and M. R. Philips.** 2007. The lymphocyte function-associated antigen-1 receptor co-stimulates plasma membrane Ras via phospholipase D2. Nat. Cell Biol. **9:**713–719.
26. **Mor, A., and M. R. Philips.** 2006. Compartmentalized Ras/MAPK signaling. Annu. Rev. Immunol. **24:**771–800.
27. **Morrison, D. K.** 2001. KSR: a MAPK scaffold of the Ras pathway? J. Cell Sci. **114:**1609–1612.
28. **Morrison, D. K., and R. J. Davis.** 2003. Regulation of MAP kinase signaling modules by scaffold proteins in mammals. Annu. Rev. Cell Dev. Biol. **19:**91–118.
29. **Muller, J., A. M. Cacace, W. E. Lyons, C. B. McGill, and D. K. Morrison.** 2000. Identification of B-KSR1, a novel brain-specific isoform of KSR1 that functions in neuronal signaling. Mol. Cell. Biol. **20:**5529–5539.
30. **Nguyen, A., W. R. Burack, J. L. Stock, R. Kortum, O. V. Chaika, M. Afkarian, W. J. Muller, K. M. Murphy, D. K. Morrison, R. E. Lewis, J. McNeish, and A. S. Shaw.** 2002. Kinase suppressor of Ras (KSR) is a scaffold which facilitates mitogen-activated protein kinase activation in vivo. Mol. Cell. Biol. **22:**3035–3045.
31. **Nosaka, T., T. Kawashima, K. Misawa, K. Ikuta, A. L. Mui, and T. Kitamura.** 1999. STAT5 as a molecular regulator of proliferation, differentiation and apoptosis in hematopoietic cells. EMBO J. **18:**4754–4765.
32. **Ohmachi, M., C. E. Rocheleau, D. Church, E. Lambie, T. Schedl, and M. V. Sundaram.** 2002. C. elegans ksr-1 and ksr-2 have both unique and redundant functions and are required for MPK-1 ERK phosphorylation. Curr. Biol. **12:**427–433.
33. **Orange, J. S.** 18 August 2008, posting date. Formation and function of the lytic NK-cell immunological synapse. Nat. Rev. Immunol. [Epub ahead of print.] doi:10.1038/nri2381.
34. **Orange, J. S., K. E. Harris, M. M. Andzelm, M. M. Valter, R. S. Geha, and J. L. Strominger.** 2003. The mature activating natural killer cell immunologic synapse is formed in distinct stages. Proc. Natl. Acad. Sci. USA **100:**14151–14156.
35. **Ory, S., M. Zhou, T. P. Conrads, T. D. Veenstra, and D. K. Morrison.** 2003. Protein phosphatase 2A positively regulates Ras signaling by dephosphorylating KSR1 and Raf-1 on critical 14-3-3 binding sites. Curr. Biol. **13:**1356–1364.
36. **Perez de Castro, I., T. G. Bivona, M. R. Philips, and A. Pellicer.** 2004. Ras activation in Jurkat T cells following low-grade stimulation of the T-cell receptor is specific to N-Ras and occurs only on the Golgi apparatus. Mol. Cell. Biol. **24:**3485–3496.
37. **Plowman, S. J., and J. F. Hancock.** 2005. Ras signaling from plasma membrane and endomembrane microdomains. Biochim. Biophys. Acta **1746:**274–283.
38. **Prior, I. A., and J. F. Hancock.** 2001. Compartmentalization of Ras proteins. J. Cell Sci. **114:**1603–1608.
39. **Raabe, T., and U. R. Rapp.** 2002. KSR—a regulator and scaffold protein of the MAPK pathway. Sci. STKE **2002:**PE28.
40. **Razidlo, G. L., R. L. Kortum, J. L. Haferbier, and R. E. Lewis.** 2004. Phosphorylation regulates KSR1 stability, ERK activation, and cell proliferation. J. Biol. Chem. **279:**47808–47814.
41. **Rechavi, O., I. Goldstein, H. Vernitsky, B. Rotblat, and Y. Kloog.** 2007. Intercellular transfer of oncogenic H-Ras at the immunological synapse. PLoS ONE **2:**e1204.
42. **Robertson, L. K., L. R. Mireau, and H. L. Ostergaard.** 2005. A role for phosphatidylinositol 3-kinase in TCR-stimulated ERK activation leading to paxillin phosphorylation and CTL degranulation. J. Immunol. **175:**8138–8145.
43. **Rocheleau, C. E., K. Cullison, K. Huang, Y. Bernstein, A. C. Spilker, and M. V. Sundaram.** 2008. The Caenorhabditis elegans ekl (enhancer of ksr-1 lethality) genes include putative components of a germline small RNA pathway. Genetics **178:**1431–1443.
44. **Roy, F., G. Laberge, M. Douziech, D. Ferland-McCollough, and M. Therrien.** 2002. KSR is a scaffold required for activation of the ERK/MAPK module. Genes Dev. **16:**427–438.
45. **Sacks, D. B.** 2006. The role of scaffold proteins in MEK/ERK signalling. Biochem. Soc. Trans. **34:**833–836.
46. **Shaul, Y. D., and R. Seger.** 2007. The MEK/ERK cascade: from signaling specificity to diverse functions. Biochim. Biophys. Acta **1773:**1213–1226.
47. **Stefanova, I., B. Hemmer, M. Vergelli, R. Martin, W. E. Biddison, and R. N. Germain.** 2003. TCR ligand discrimination is enforced by competing ERK positive and SHP-1 negative feedback pathways. Nat. Immunol. **4:**248–254.
48. **Stinchcombe, J. C., G. Bossi, S. Booth, and G. M. Griffiths.** 2001. The immunological synapse of CTL contains a secretory domain and membrane bridges. Immunity **15:**751–761.
49. **Stinchcombe, J. C., and G. M. Griffiths.** 2003. The role of the secretory immunological synapse in killing by $CD8^+$ CTL. Semin. Immunol. **15:**301–305.
50. **Stinchcombe, J. C., E. Majorovits, G. Bossi, S. Fuller, and G. M. Griffiths.** 2006. Centrosome polarization delivers secretory granules to the immunological synapse. Nature **443:**462–465.
51. **Sundaram, M., and M. Han.** 1995. The C. elegans ksr-1 gene encodes a novel Raf-related kinase involved in Ras-mediated signal transduction. Cell **83:**889–901.
52. **Sundaram, M., J. Yochem, and M. Han.** 1996. A Ras-mediated signal transduction pathway is involved in the control of sex myoblast migration in Caenorhabditis elegans. Development **122:**2823–2833.
53. **Therrien, M., H. C. Chang, N. M. Solomon, F. D. Karim, D. A. Wassarman, and G. M. Rubin.** 1995. KSR, a novel protein kinase required for RAS signal transduction. Cell **83:**879–888.
54. **Trambas, C. M., and G. M. Griffiths.** 2003. Delivering the kiss of death. Nat. Immunol. **4:**399–403.
55. **Watts, J. D., J. S. Sanghera, S. L. Pelech, and R. Aebersold.** 1993. Phosphorylation of serine 59 of p56lck in activated T cells. J. Biol. Chem. **268:**23275–23282.
56. **Wei, S., A. M. Gamero, J. H. Liu, A. A. Daulton, N. I. Valkov, J. A. Trapani, A. C. Larner, M. J. Weber, and J. Y. Djeu.** 1998. Control of lytic function by mitogen-activated protein kinase/extracellular regulatory kinase 2 (ERK2) in a human natural killer cell line: identification of perforin and granzyme B mobilization by functional ERK2. J. Exp. Med. **187:**1753–1765.
57. **Winkler, D. G., I. Park, T. Kim, N. S. Payne, C. T. Walsh, J. L. Strominger, and J. Shin.** 1993. Phosphorylation of Ser-42 and Ser-59 in the N-terminal region of the tyrosine kinase $p56^{lck}$. Proc. Natl. Acad. Sci. USA **90:**5176–5180.
58. **Yachi, P. P., J. Ampudia, T. Zal, and N. R. Gascoigne.** 2006. Altered peptide ligands induce delayed CD8-T cell receptor interaction—a role for CD8 in distinguishing antigen quality. Immunity **25:**203–211.
59. **Yu, W., W. J. Fantl, G. Harrowe, and L. T. Williams.** 1998. Regulation of the MAP kinase pathway by mammalian Ksr through direct interaction with MEK and ERK. Curr. Biol. **8:**56–64.
60. **Zhou, M., D. A. Horita, D. S. Waugh, R. A. Byrd, and D. K. Morrison.** 2002. Solution structure and functional analysis of the cysteine-rich C1 domain of kinase suppressor of Ras (KSR). J. Mol. Biol. **315:**435–446.